Journal of Molecular Catalysis A: Chemical 344 (2011) 153–160

Contents lists available at ScienceDirect

Journal of Molecular Catalysis A: Chemical

journal homepage: www.elsevier.com/locate/molcata

Ru promoted cobalt catalyst on γ-Al_2O_3 support: Influence of pre-synthesized nanoparticles on Fischer–Tropsch reaction

Jo-Yong Park, Yun-Jo Lee*, Prashant R. Karandikar, Ki-Won Jun**, Jong Wook Bae, Kyoung-Su Ha

Alternative Chemicals/Fuel Research Center, Korea Research Institute of Chemical Technology, P.O. Box 107, Yusong, Daejon 305-600, South Korea

ARTICLE INFO

Article history:
Received 25 February 2011
Received in revised form 23 May 2011
Accepted 24 May 2011
Available online 31 May 2011

Keywords:
$CoRuO_x$ nanoparticles
Pre-synthesis
Ru promoter
$CoRu/Al_2O_3$ catalyst
FT synthesis

ABSTRACT

Effects of Ru promoted cobalt oxide nanoparticles on γ-Al_2O_3 supported catalysts were studied for Fischer–Tropsch reaction. Homogeneously sized cobalt oxide nanoparticles with the different amount of ruthenium promoter were prepared by solvothermal method using oleic acid as capping agent. Pre-synthesized $CoRuO_x$ nanoparticles were then impregnated on γ-Al_2O_3 support to prepare 5CoxRu/100Al_2O_3 catalysts (5CoxRuAl), with the amount of ruthenium $x = 0$ to 0.1. The catalysts were characterized by XRD, TEM, TPR, EDX, H_2 chemisorption and O_2 titration methods and compared with the catalyst prepared by conventional impregnation method, i.e. i-5Co0.05RuAl. Interestingly, catalysts prepared by nanoparticle impregnation method showed higher H_2 uptake and better reducibility with the concomitant increase in the activity due to the homogeneous dispersion of the Ru promoter across entire the nanoparticles as compared to the catalyst prepared by conventional impregnation method. The intimate contact between cobalt and ruthenium enhanced the site density of cobalt which was responsible for the promotional results in the case of 5CoxRuAl catalysts.

1. Introduction

In recent years, Fischer–Tropsch synthesis (FTS) has gained tremendous importance due to the green environmental requirements, which limits the residual sulfur between 30 and 50 ppm in diesel fuel. Cobalt- or iron-based catalysts normally show excellent activity for syngas conversion to petroleum products leading to super clean diesel fuels with low sulfur and aromatics contents. Generally, cobalt-based catalysts are preferred for the FTS due to the high activity and selectivity towards long chain hydrocarbons [1–3]. Due to the low water gas shift (WGS) activity, cobalt based catalysts are most preferred catalysts in GTL (gas-to-liquids) technology for the production of diesel [1].

The activity of Co-based FT catalyst depends upon the particle size of metal, loading amounts with respect to support, reduction degree, metal dispersion and support-active metal interaction. High cobalt loading, up to about 30% is reported in commercial catalysis for FTS, which is very high as compared to the noble metal promoted cobalt based catalysts [2]. Noble metals such as Ru, Pt, and Re have been employed with Co-based catalysts in order to increase the reduction degree of cobalt. There are reports describing the use of small amount of noble metals along with cobalt oxide to enhance the reduction degree almost two-fold more than without using promoter elements [2]. In addition, promoters also help in controlling the particle size of the reduced metal clusters [3]. It has been shown that the presence of Ru as a promoter enhances the interaction between Co and Ru, thus the presence of noble metal led to bimetallic crystallite formation which is an excellent approach to decrease the reduction temperature [4,5]. Iglesia [6] reported ruthenium as a structural promoter for Co-based catalysts which also prevents the agglomeration of cobalt oxide particles during calcination. Xiong et al. [7] studied the effect of Ru content on Co/SBA-15 catalyst for FT activity, where they used the conventional synthesis procedure for the preparation of catalyst by co-impregnation of an aqueous solution of cobalt nitrate and ruthenium nitrosyl nitrate. Similar study have been performed by Li et al. [8] who reported that the small amount of Ru offers an excellent performance in lowering the reduction temperature of cobalt oxide to cobalt metallic species.

There are many reports on the promoted cobalt catalysts for FT synthesis, suggesting the preparation of catalyst using traditional impregnation methods [1,5,7,10–14]. However the advantage of controlled particles size may not be possible and the particles with the broad range of crystal size may appear in the catalyst. In this context Lee et al. [9] reported the preparation of size controlled Co_3O_4 nanoparticles on alumina support and obtained high CO conversion as compared to the catalysts prepared using conventional impregnation and precipitation methods. The advantage of controlled nanocrystal deposition can be enhanced by the addition

* Corresponding author. Tel.: +82 42 860 7630; fax: +82 42 860 7388.
** Corresponding author. Tel.: +82 42 860 7671; fax: +82 42 860 7388.
E-mail addresses: yjlee@krict.re.kr (Y.-J. Lee), kwjun@krict.re.kr (K.-W. Jun).

1381-1169/$ – see front matter © 2011 Elsevier B.V. All rights reserved.
doi:10.1016/j.molcata.2011.05.022

of small amount of promoter which increase the dispersion and reducibility of active metal and achieve improved conversion and selectivity. Intimate contact between the promoter element and the active metal is most essential to acquire the advantage of bimetallic synergy. In this regards here we are reporting the preparation of 5CoxRuAl catalysts by impregnation method of pre-synthesized CoRuOx nanoparticles of controlled. The catalysts thus prepared, show less-agglomerated spherical particles even after calcination. By adopting the above methodology, it is expected that the dispersion of cobalt on the catalyst support will be better due to the intimate contact between Co and Ru, and the presence of ruthenium promoter will reduce cobalt oxide comparatively at lower reduction temperature.

2. Experimental

2.1. Synthesis of $CoRuO_x$ nanoparticles

CoRuOx nanoparticles with the different amount of ruthenium were synthesized by solvothermal method [1] so as to obtain the final catalyst with 5% cobalt and the ruthenium content from 0 to 0.1%. In brief, $CoRuO_x$ nanoparticles were prepared by using CoRu-oleate precursor which was synthesized from cobalt chloride, ruthenium chloride, oleic acid and NH_3 (30%) solution. CoRu-oleate precursor was heated to 230 °C for 3 h in 1-octadecene. After cooling to room temperature, the material was collected by repeated washing with acetone and finally air-dried to obtain $CoRuO_x$ nanoparticles. These pre-synthesized $CoRuO_x$ nanoparticles were dispersed in hexane.

2.2. Catalyst preparation

γ-Al_2O_3 (surface area of 294.5 m^2/g) supported $CoRuO_x$ nanoparticles with the weight ratio of Co:Ru:Al_2O_3 = 5:0–0.1:100 were prepared by impregnation method using dispersed $CoRuO_x$ nanoparticle solution in hexane from Section 2.1 and according to the reported procedure [9]. The catalysts were designated as 5CoxRuAl (where x varies from 0 to 0.1). For comparison, 5Co0.05Ru/100Al_2O_3 catalyst was also prepared by impregnation of cobalt chloride and ruthenium chloride solutions over γ-Al_2O_3 and the sample was denoted as i-5Co0.05RuAl. The prepared catalysts were dried at 60 °C for 12 h, followed by calcination at 400 °C for 5 h in static air.

2.3. Catalyst characterization

The $CoRuO_x$ nanoparticles and 5CoxRuAl catalysts were characterized by X-ray diffraction (XRD) measurement on a Rigaku D/MAX-2200V diffractometer using Cu/Kα radiations (λ = 0.154056 nm). $CoRuO_x$ nanoparticles were studied for their morphology by using the transmission electron microscopy (TEM; TECNAI G20 instrument) operating at 200 kV, together with energy dispersive X-ray (EDX) analysis. The prepared catalysts were subjected to the temperature programmed reduction (TPR) studies and the reduction profiles were obtained using a Micromeritics TPR equipped with a thermal conductivity detector (TCD). The samples were pretreated in helium flow at 200 °C for 2 h to remove the adsorbed water. The catalysts were passed over 5% H_2/Ar reducing gas at the flow rate of 30 cm^3/min and heated from 100 to 1000 °C at the heating rate of 10 °C/min and maintained at final temperature for 30 min. The cobalt dispersion of 5CoxRuAl catalysts was measured by H_2 chemisorption and O_2 titration using Micrometrics ASAP 2020C instrument. The sample was reduced in situ at 350 °C for 10 h and then cooled to 100 °C. After the hydrogen chemisorption, the sample was re-oxidized at 400 °C by 10% O_2 in helium to determine the extent of reduction. Percentage dispersion (D%) of the cobalt metal was calculated according to the following equation [4,6],

$$D\% = \frac{1.179X}{Wf}$$

where X (μmol/g) is the total H_2 uptake, W is the weight percentage of cobalt and f is the fraction of Co reduced to metal, determined by O_2 titration. Average particle size (dp (nm)) was calculated from D% assuming spherical metal crystallite of uniform diameter by the equation, dp = 96/D%.

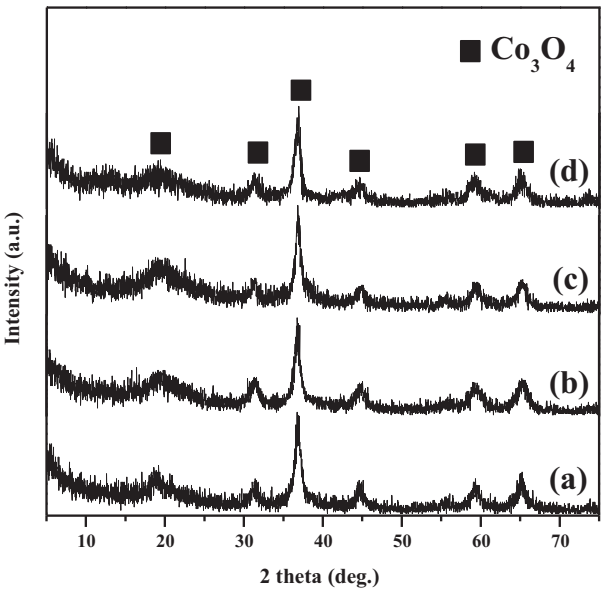

Fig. 1. XRD patterns of the $CoRuO_x$ nanoparticles: (a) 5Co, (b) 5Co0.025Ru, (c) 5Co0.05Ru, and (d) 5Co0.1Ru.

2.4. Activity test

For FTS, 5CoxRuAl catalysts were tested in a tubular fixed bed reactor and compared with the conventional i-5Co0.05RuAl catalyst. For the reaction, 0.5 g of catalyst was reduced in flowing 5% H_2/Ar (200 cm^3/min) at 350 °C for 10 h. The activity test was conducted under the following reaction conditions; T = 220 and 240 °C; Pg = 10 kgf/cm^2; SV (L/kg_{cat}/h) = 3600; feed compositions (H_2/CO/Ar; mol%) = 63.0/31.5/5.5.

3. Results and discussion

3.1. Analysis of $CoRuO_x$ nanoparticles

As-synthesized $CoRuO_x$ nanoparticles with the different amount of Ru are characterized by X-ray diffraction (XRD) in Fig. 1. XRD shows similar pattern to that of pure Co_3O_4 with the peaks at around 2θ = 31°, 37°, 38.5°, 45° and 59.5° which indicate the presence of face-centered cubic cobalt oxide. The sizes of $CoRuO_x$ nanoparticles determined by Scherrer equation from the most intense Co_3O_4 peak at around 2θ = 37° are summarized in Table 1. In the previous reports [11,15], when the catalyst was prepared by Ru doping via impregnation of respective ions, prominent XRD peak for RuO_2 was observed along with the reduction in the particle size of cobalt oxide. Here we observe the decrease in the particle size of cobalt oxide with the increase in the Ru content; however we do not observe any peak for RuO_2 promoter in the XRD pattern. The intensity of RuO_2 depends upon the amount of ruthenium as well as its particle size, and peaks for crystallite below 5 nm which is lower than the X-ray detectable limit will not appear in the spectra

Table 1
Physisorption data and particles size of 5CoxRuAl catalysts.

Sample	Surface area (m^2/g)	Average pore diameter (nm)	Pore volume (cm^3/g)	Particle size by XRD (nm)	
				$CoRuO_x$	5CoxRuAl catalyst
γ-Al_2O_3	294.5	24.5	1.81	–	–
5CoAl	264.2	25.5	1.68	14.2	21.9
5Co0.025RuAl	279.4	24.7	1.73	13.7	18.3
5Co0.05RuAl	280.5	24.1	1.69	13.6	17.7
5Co0.1RuAl	282.2	21.7	1.54	12.1	14.7

[15]. This shows that ruthenium is well dispersed on the catalyst surface with the crystallite smaller than 5 nm. Due to the better dispersion, the number of ruthenium atoms in the vicinity of cobalt are increased which is ultimately beneficial for the reducibility of cobalt.

TEM images are used to illustrate the structural information of $CoRuO_x$ nanoparticles as shown in Fig. 2. With the increase in the ruthenium content, flowerlike shape of $CoRuO_x$ nanoparticles become distinct with the slight reduction in the particles size. The results for crystal size in TEM are similar to XRD data (Table 1) with the variation of the cobalt nanoparticles size between 12 and 14 nm.

3.2. Analysis of cobalt catalysts

The textural properties of 5CoxRuAl catalysts prepared by using pre-synthesized $CoRuO_x$ nanoparticles are shown in Table 1. Surface area and pore volume of γ-Al_2O_3 decrease with the impregnation of cobalt oxide nanoparticles, which shows the deposition of nanoparticles within the porous support. However, the pore diameter of catalysts remain almost constant which indicate that the pores are not blocked due to the impregnation. It is observed that with the increase in the ruthenium content, surface area increases which may be due to the decrease in the particle size of cobalt oxide.

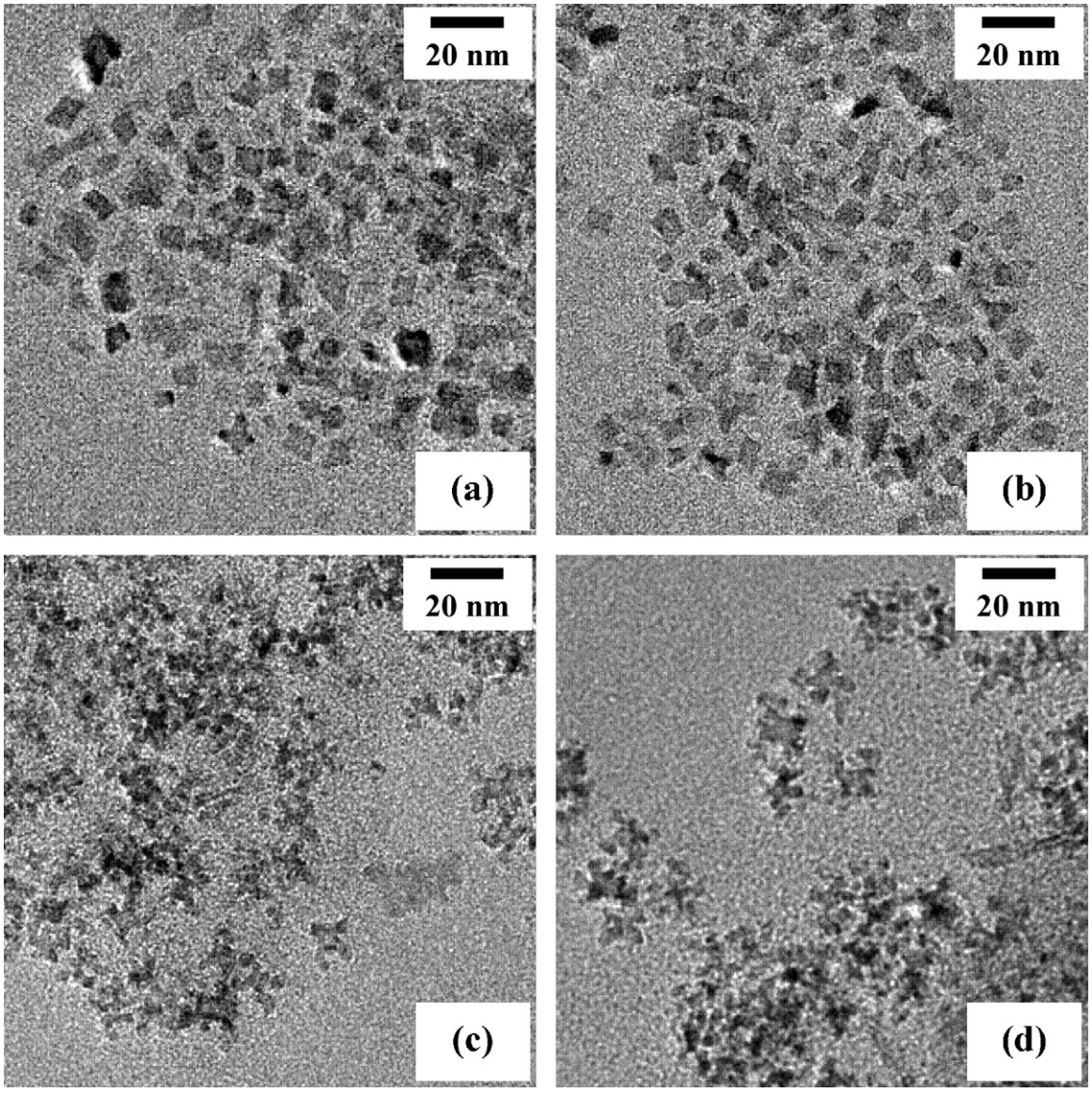

Fig. 2. TEM images of the $CoRuO_x$ nanoparticles: (a) 5Co, (b) 5Co0.025Ru, (c) 5Co0.05Ru, and (d) 5Co0.1Ru.

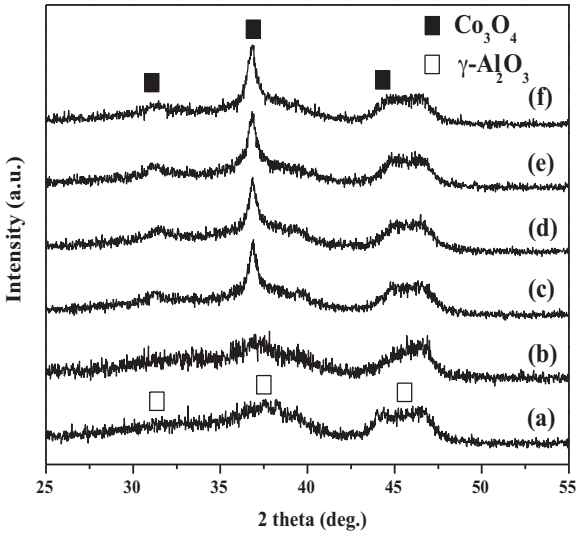

Fig. 3. XRD patterns of (a) γ-Al_2O_3, (b) i-5Co0.05RuAl, (c) 5CoAl, (d) 5Co0.025RuAl, (e) 5Co0.05RuAl, and (f) 5Co0.1RuAl.

XRD profiles for all the 5CoxRuAl catalysts show diffraction pattern for Co_3O_4 irrespective of the variation in the Ru content (Fig. 3(c)–(f)). The major diffraction peaks at $2\theta = 31^\circ, 37^\circ, 38.5^\circ$ and 45° indicating the existence of Co_3O_4 spinal phase [8]. The difference between 5CoxRuAl catalysts and bare $CoRuO_x$ nanoparticles in the XRD patterns is obvious in terms of reduction in the intensities of all the reflections. Such reduction in the peak intensities are due to the dispersion of metal particles within the amorphous support with high surface area and porosity. XRD pattern for i-5Co0.05RuAl catalyst is very broad as shown in Fig. 3(b) which indicates the smaller crystal size. However, these broad peaks of cobalt oxide are overlapped with the peaks of γ-alumina. Thus the size of cobalt oxide is difficult to determine and not mentioned in Table 1. Comparative study of the size of $CoRuO_x$ nanoparticles using XRD, before and after impregnation on the support showed that the crystal size increases after catalyst formation. This shows some amount of agglomeration of metal during catalyst preparation. When pre-synthesized cobalt oxide nanoparticles are impregnated without the addition of promoter (5CoAl), the effect of agglomeration is more pronounced. Interestingly, with the addition of increasing amount of ruthenium promoter, agglomeration decreases considerably due to the dispersion of cobalt and the difference between the sizes of pre-synthesized and impregnated nanoparticles reduces. Kogelbauer et al. [11] previously reported the decrease in the particle size and increase in the dispersion of cobalt with the addition of Ru promoter.

TEM images of 5CoxRuAl catalysts are shown in Fig. 4. The images show the spherical-shaped $CoRuO_x$ nanoparticles which are dispersed on the rod- and plate-shaped alumina for all the 5CoxRuAl catalysts (Fig. 4(b)–(e)). The particles size of the $CoRuO_x$ nanoparticles decreases from about 22 to 14 nm with the increase in the Ru content in the catalysts. However 5CoxRuAl catalysts show comparatively uniform $CoRuO_x$ nanoparticles, mono-dispersed on alumina with respect to i-5Co0.05RuAl catalyst which is shown in Fig. 4(a).

The distribution of Ru particles alongside cobalt in the case of nanoparticles impregnated catalysts i.e. 5CoxRuAl is confirmed by energy-dispersive X-ray spectrometry (EDX). Fig. 5 shows the EDX mapping of representative sample 5Co0.05RuAl. EDX of one of the particles site shows the presence of cobalt (0.7, 6.9 and 7.7 keV) and Ru particles (2.6 keV) in the close vicinity. The result gives the clear evidence for the intimate contact between Co and Ru particles in the catalyst. Similarly in the previous report Tsubaki et al. [16] showed the formation of Co–Ru bimetallic particles using EDX analysis.

TPR was performed to determine the reduction behavior of the catalysts (Fig. 6). TPR profile of unprompted 5CoAl catalyst (Fig. 6(b)) shows two reduction peaks; first reduction peak at 360 °C assigned to the reduction of Co_3O_4 to CoO, and CoO to cobalt metal and the second peak at 590 °C assigned to the reduction of cobalt species interacting with the support [3,11]. It is appropriate to propose that, since ruthenium oxide can be reduced at lower temperatures than cobalt oxide, metallic ruthenium could act as reduction nuclei via smooth spreading of hydrogen over the cobalt species [17]. Hence for Ru promoted catalysts i.e. 5Co0.025RuAl and 5Co0.05RuAl, the reduction peaks shifted from 360 °C to 285 °C and from 590 °C to 500 °C (Fig. 6(c) and (d)) as compared to 5CoAl due to the presence of promoter which reduce the interaction of cobalt oxide with the support and enhance the reducibility of cobalt oxide. However, at the higher loading of the promoter up to 0.1% there is no further shift in the reduction peak for 5Co0.1RuAl catalyst. Instead, we observe peak at 170 °C (Fig. 6(e)) due to the reduction of ruthenium oxide to ruthenium metal [15]. The increase in the Ru loading up to 0.1 wt% results in the segregation of RuO_2 from the surface of Co_3O_4 particle [12], hence reduction behavior of 5Co0.1RuAl catalyst does not change. These results show that the addition of ruthenium leads to easy reduction of cobalt oxide to metallic cobalt for 5CoxRuAl catalysts up to the ruthenium amount of 0.05%. These results are consistent with the earlier reports which showed that the promotion of noble metals resulted in the significant decrease in catalyst reduction temperature [1,3–5,15–18]. TPR profile for i-5Co0.05RuAl catalyst shows little influence of promoter on the reducibility of Co_3O_4 (Fig. 6(a)) compared to that of 5CoAl. This is due to the random distribution of Ru with respect to cobalt oxide and alumina support which resulted in the small influence on the first reduction peak with no effect on the reduction temperature of second peak. Compared to 5Co0.05RuAl, the reduction peaks of i-5Co0.05RuAl is broader and shifted to higher temperature which is due to smaller crystal size by different preparation method.

H_2 chemisorption results show that the addition of ruthenium causes more than four times higher H_2 uptake for 5Co0.1RuAl catalyst as compared to unpromoted 5CoAl catalyst (Table 2). This is due to the increase in the dispersion and decrease in the particles size of cobalt metal with the increasing amount of promoter. It is also observed that the values for O_2 uptake and percentage reduction increase with the increase in ruthenium content for 5CoxRuAl catalysts. However, 5Co0.1RuAl catalyst exhibited lower O_2 uptake and reduction degree as compared to 5Co0.05RuAl catalyst which is due to the segregation of RuO_2 from the surface of Co_3O_4 [12]. Based on the above discussion, it is determined that the addition of ruthenium promoter improves the reducibility and H_2 adsorption of cobalt oxide which is essential to enhance the catalytic activity. In the case of i-5Co0.05RuAl catalyst, the lower values for O_2 uptake and H_2 chemisorption as compared to nanoparticles-impregnated catalysts are due to the random distribution of promoter with respect to cobalt and broad cobalt particle size distribution. This gives rise to the lower Co–Ru bimetallic synergy. 5Co0.05RuAl catalyst shows higher values for H_2 chemisorption, O_2 uptake and ultimately reduction degree as compared to the other catalysts. Ru-promoted cobalt catalyst with pre-synthesized $CoRuO_x$ nanoparticles gives rise to higher degree of reducibility due to the enhanced cobalt–ruthenium bimetallic influence and reduced cobalt–support interaction. The particle size of Co metals in the reduced catalysts is estimated by H_2 chemisorption. The values are first calculated based on the total metal loading, but corrected by subsequently taking the degree of reducibility into consideration. The chemisorption data reveal the decrease in the Co particle size with the addition of ruthenium which is in accordance with the

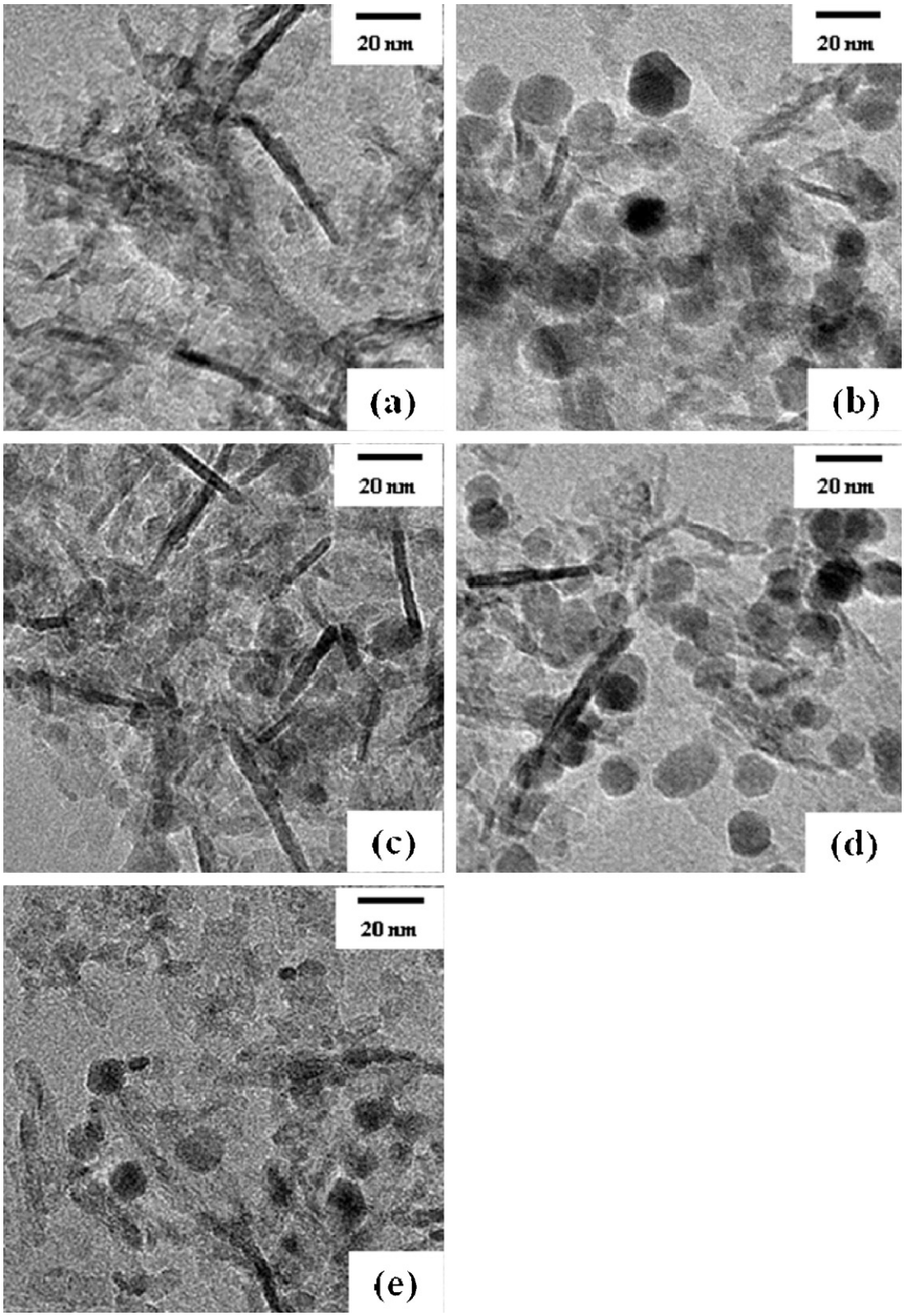

Fig. 4. TEM images of (a) i-5Co0.05RuAl, (b) 5CoAl, (c) 5Co0.025RuAl, (d) 5Co0.05RuAl, and (e) 5Co0.1RuAl.

XRD results. However in the case of i-5Co0.05RuAl catalyst prepared by conventional method, difference is observed in the cobalt crystal size estimated by XRD and H_2 chemisorption method. i-5Co0.05RuAl catalyst may have broad range of cobalt crystal size distribution with majority of small crystals which is due to the lower amount of cobalt loading as seen from XRD pattern. The smaller cobalt oxide particles can give stronger interaction with the support due to its higher contact area with support which gives rise to difficultly reducible cobalt oxide species as verified from TPR profile. Furthermore the random distribution of Ru promoter on both

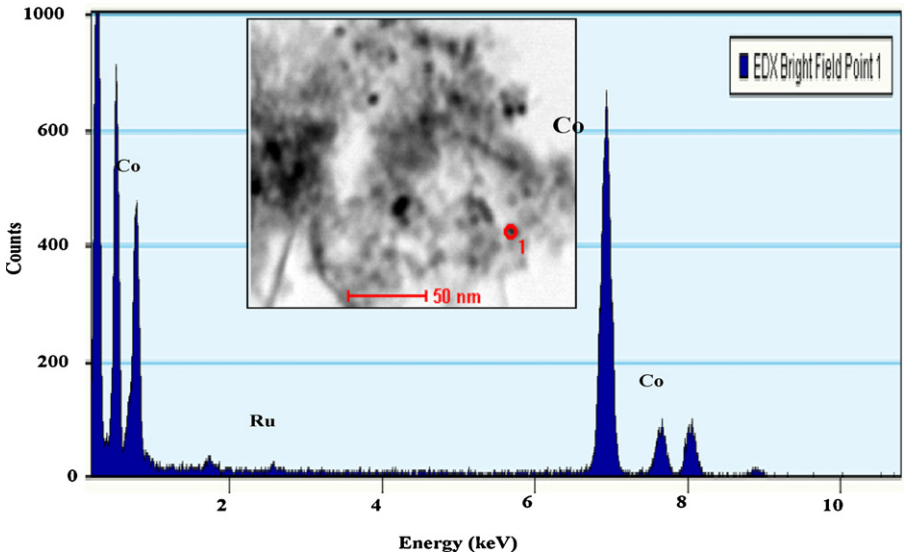

Fig. 5. EDX spectrum of 5Co0.05RuAl catalyst.

Table 2
H_2 chemisorption and O_2 titration result for $CoRu/Al_2O_3$ catalysts.

Sample	H_2 uptake (μmol/g)	Uncorrected dispersion (%)[a]	Uncorrected Co diameter (nm)[b]	O_2 uptake (μmol/g)	Reduction degree (%)[c]	Corrected dispersion (%)[d]	Corrected Co diameter (nm)[e]
i-5Co0.05RuAl	6.8	1.7	56.1	187	35.3	4.8	19.8
5CoAl	5.4	1.4	70.6	165	31.2	4.4	22.0
5Co0.025RuAl	12.8	3.2	29.8	294	55.5	5.8	16.5
5Co0.05RuAl	19.1	4.8	20.2	421	79.5	6.0	15.9
5Co0.1RuAl	22.9	5.8	16.7	409	77.2	7.5	12.9

[a] Dispersion (D) = surface Co^0 atom/total Co atom × 100, assumed stoichiometric adsorption ratio of $H_2/Co = 1/2$.
[b] Co particle size calculated from H_2 chemisorptions using d (Co) = 96/D.
[c] Calculated from O_2 uptake.
[d] Corrected dispersion (D) = surface Co^0 atom/total reduced Co^0 atom × 100 = surface Co^0 atom/(total Co atom × reduced fraction) × 100.
[e] Corrected Co diameter = uncorrected Co diameter × reduced Co fraction.

cobalt oxide and support in the i-5Co0.05RuAl catalyst may not help the reduction of cobalt oxide. Thus only few big crystals existing in i-5Co0.05RuAl catalyst are reducible and show large value of cobalt crystal size in the chemisorption data as compared to the XRD results.

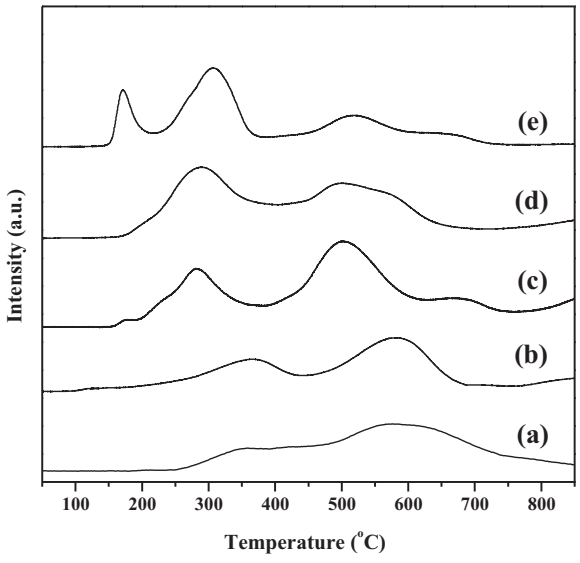

Fig. 6. TPR profiles of (a) i-5Co0.05RuAl, (b) 5CoAl, (c) 5Co0.025RuAl, (d) 5Co0.05RuAl, and (e) 5Co0.1RuAl.

3.3. FT activity test

The activities of 5CoxRuAl catalysts along with i-5Co0.05RuAl, after reduction at 350 °C/10 h, are measured in a fixed bed reactor at 220 and 240 °C and summarized in Tables 3 and 4, respectively. The trends of activities of the 5CoxRuAl catalysts at 220 °C are similar to the results obtained at 240 °C, although all the catalysts show higher conversion and selectivity at 240 °C as compared to their respective values at 220 °C. CO_2 formation is absent for all the catalysts at 220 °C and is negligible at 240 °C. This is due to the low water gas shift (WGS) activity on cobalt based catalysts. At the reaction temperature of 220 °C, 5Co0.05RuAl catalyst shows higher CO conversion of 22.1% as compared to other catalysts (Table 3). As discussed before, 5Co0.05RuAl catalyst shows better dispersion of metal with nearly uniform cobalt particles and higher degree of reducibility at lower temperature which is responsible for higher activity. At the temperature of 240 °C, similar trends of activities are observed (Table 4) and the most active 5Co0.05RuAl catalyst has showed the CO conversion of 57%. In the case of 5Co0.1RuAl catalyst even though the amount of promoter is higher i.e. 0.1%, the activity decreases. The addition of increasing amount of Ru promoter in the case of 5CoxRuAl catalysts gives rise to the decrease in the cobalt particle size and increase in the dispersion as shown in Table 2. Hence we observed the higher H_2 uptake value in the case of 5Co0.1RuAl catalyst. However there is no difference in the TPR profile and reducibility results in the case of 5Co0.1RuAl as compared to 5Co0.05RuAl catalyst. This is mainly due to the segregation of RuO_2 from the surface of Co_3O_4 particle above certain optimum concentration of ruthenium promoter. The influence of Ru segre-

Table 3
CO conversion and products distribution result for $CoRu/Al_2O_3$ catalysts.

Sample no.	Conversion (%)		Hydrocarbon selectivity (%)			$O/(O+P) \times 100$ in C_2–C_4
	CO	To CO_2	CH_4	C_2–C_4	C_{5+}	
i-5Co0.05RuAl	2.2	0	10.6	12.1	77.3	68.9
5CoAl	1.5	0	13.6	11.2	75.2	70.3
5Co0.025RuAl	14.6	0	10.9	10.5	78.6	67.8
5Co0.05RuAl	22.1	0	10.3	9.6	79.1	60.0
5Co0.1RuAl	17.2	0	10.1	8.4	81.5	58.0

Reaction conditions: $T = 220\,^{\circ}C$; $Pg = 10\,kgf/cm^2$; SV ($L/kg_{cat}/h$) = 3600; feed compositions ($H_2/CO/Ar = 63.0/31.5/5.5$; mol%); TOS = 30 h.

gation on TPR profile in the case of 5Co0.1RuAl catalyst is already discussed in the manuscript. Song et al. [12] previously reported the effect of Ru segregation on the alumina supported cobalt catalyst for FT reaction. Similarly, catalytic activity in FTS depends upon the two factors, cobalt dispersion and reduction degree. Higher dispersion decreases the cobalt particles size and the particles size below certain optimum value of 8 nm cause sharp decrease in the catalyst activity [19]. However in the case of 5Co0.1RuAl catalyst, particle size of cobalt is more than 12 nm which is controlled by using appropriate capping agent. Hence the effect of higher dispersion is expected to play an important role in the catalyst activity. In spite of this, the effect of lower reducibility of 5Co0.1RuAl catalyst due to the segregation of promoter overcomes the influence of dispersion, hence shows decrease in the conversion (41%) as compared to 5Co0.05RuAl catalyst.

The rate of CH_4 formation is higher in the case of 5CoAl catalyst due to the lower reducibility of cobalt oxide particles. The addition of increasing amount of promoter increases the reducibility and decreases CH_4 formation in 5CoxRuAl catalysts for both the reaction temperatures. However there is not much difference in the methane selectivity for i-5Co0.05RuAl and 5CoxRuAl catalysts. In the case of i-5Co0.05RuAl catalyst, possibility of uneven particle size distribution is very high as compared to the size controlled cobalt particles in the case of 5CoxRuAl catalysts. Difficultly reducible small cobalt crystals in the case of i-5Co0.05RuAl catalyst are mostly exists in oxide phase during FTS. Hence product selectivity is governed by the bigger crystals within broad range of size distributed cobalt particles. Thus we observed that methane selectivity is almost similar for all the catalysts even though overall activity of 5CoxRuAl catalysts is very high due to the uniform cobalt particles distribution and there intimate interaction with the promoter.

It is observed that, C_{5+} selectivity increases at the expenses of C_2–C_4 hydrocarbons with increase in the ruthenium concentration in the catalysts from 0 to 0.1 wt%. There are many reports about the increase in C_{5+} selectivity with the increase in the particles size of cobalt which is due to the easier dissociation of CO, leading to the possible secondary reaction of olefins through chain growth mechanism [20,21]. However in the case of Ru promoted catalysts, the bimetallic interaction influences the dispersion and reducibility of supported metals which is reflected here in the results of XRD, TPR, H_2 chemisorption, etc. The cleansing effect of Ru during CO hydrogenation due to its high hydrogenation ability prevents the formation of carbon deposits on the catalyst surface. This phenomenon increases the site density of cobalt [22] which encourages the re-adsorption of α-olefins and increases the chain growth probability. In effect, Ru-promoted samples promote chain propagation by predominantly re-adsorbing lighter olefins and produce C_{5+} hydrocarbons more. Iglesia [23] previously reported the higher rate of C_{5+} hydrocarbons and paraffin in the FT synthesis is due to the promotional effect of Ru on Co/TiO_2 and Co/SiO_2 catalysts. There the bimetallic effect is obtained by the intimate contact between Co and Ru components which is induced by the high temperature calcination of Co–Ru precursors. Here, pre-synthesized nanoparticles formation causes highly organized bimetallic synergy and the synergy effect increases with the increase in the Ru content. Moreover, these changes occurred without increase in the concentration of Co. We also observe the decrease in the percentage selectivity for $O/(O+P)$ in the range of C_2–C_4 hydrocarbons with the addition of increasing amount promoter from 0 to 0.1% for both the reaction temperatures. This is due to the increase in the hydrogen uptake with the increasing amount of promoter. This gives rise to more number of active sites to catalyze hydrogenation which converts olefins to paraffins.

Comparative study of the activities for 5Co0.05RuAl and conventionally prepared i-5Co0.05RuAl catalyst shows superior results in the case of former catalyst even though the amounts of ruthenium and cobalt are the same for both the catalysts. CO conversion for 5Co0.05RuAl catalyst is ∼10 times higher at 220 °C and ∼6 times higher at 240 °C as compared to i-5Co0.05RuAl catalyst (Tables 3 and 4). This considerable difference in the activity is due to the homogeneous distribution of cobalt with ruthenium in the case of 5Co0.05RuAl catalyst. We previously reported the higher metal dispersion and reducibility for cobalt based catalyst using pre-synthesized cobalt nanoparticles [9]. To improve the metal dispersion in the case of ruthenium promoted cobalt catalyst, it is essential to synthesize nearly mono-dispersed $CoRuO_x$ nanoparticles. As shown in Fig. 7(a), the conventional process normally generates the different particle sizes of Co and Ru with the random distribution on the support. The ruthenium particles which are not in the vicinity of cobalt show no influence on the reducibility of cobalt oxide. According to the present method (Fig. 7(b)), the two-step approach is (i) preparation of $CoRuO_x$ nanoparticles with the controlled size using appropriate capping agent and (ii)

Table 4
CO conversion and products distribution result for $CoRu/Al_2O_3$ catalysts.

Sample no.	Conversion (%)		Hydrocarbon selectivity (%)			$O/(O+P) \times 100$ in C_2–C_4
	CO	To CO_2	CH_4	C_2–C_4	C_{5+}	
i-5Co0.05RuAl	9.6	0	14.5	15.8	69.7	58.1
5CoAl	3.1	0	17.9	14.5	67.6	68.2
5Co0.025RuAl	36.9	0.4	15.8	13.4	70.8	47.1
5Co0.05RuAl	57.0	1.1	14.7	12.9	72.4	44.0
5Co0.1RuAl	41.0	0.8	13.2	10.6	76.2	42.0

Reaction conditions: $T = 240\,^{\circ}C$; $Pg = 10\,kgf/cm^2$; SV ($L/kg_{cat}/h$) = 3600; feed compositions ($H_2/CO/Ar = 63.0/31.5/5.5$; mol%); TOS = 50 h.

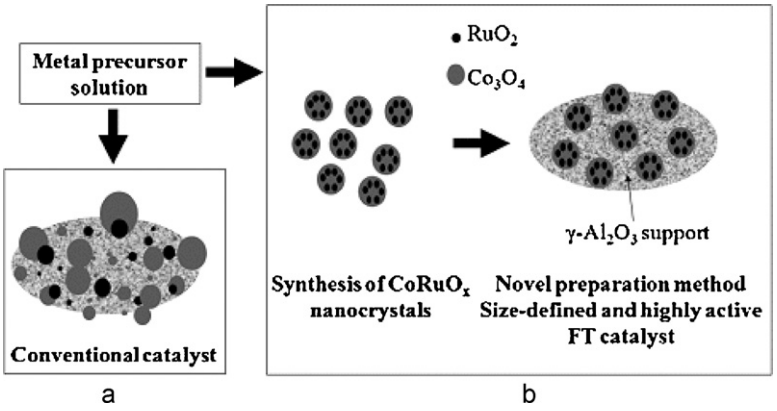

Fig. 7. Schemes for formation of $CoRuO_x$ nanoparticles and their dispersion on the support (a) conventional method and (b) present method.

homogenous distribution of the $CoRuO_x$ throughout the support maintaining uniformity as well as minimizing the possibility of separation of Ru and Co particles. Hence the impregnation of pre-synthesized $CoRuO_x$ nanoparticles in the case of 5CoxRuAl catalysts enhances synergistic effects by the formation of bimetallic Co–Ru particles with better dispersion as discussed in the EDX results. Present approach was proved by the results of TPR, H_2 chemisorption, O_2 titration and finally the activity and selectivity of 5CoxRuAl catalysts as compared to conventional catalyst.

4. Conclusions

The series of 5CoxRuAl catalysts are synthesized by using $CoRuO_x$ nanoparticles, with the ruthenium content varying from 0 to 0.1%. The Ru promoted Co catalysts show increase in the activity as compared to unpromoted 5CoAl catalyst. The activity of the catalyst improves with the amount of promoter and 5Co0.05RuAl catalyst with 0.05% promoter show excellent results. However, further increase in the Ru loading (0.1%) results in the segregation of RuO_2 from the surface of Co_3O_4 which shows detrimental effect on the conversion. Interestingly 5Co0.05RuAl catalyst shows higher activity and selectivity as compared to the conventionally prepared i-5Co0.05RuAl catalyst with the equal amounts of cobalt and ruthenium. The pre-synthesized $CoRuO_x$ nanoparticles in the case of 5CoxRuAl catalysts increase the intimate contact between cobalt and ruthenium. The synergistic effects of the catalyst by the formation of more number of bimetallic Co–Ru particles with the controlled particles size influence the FT activity and C_{5+} selectivity for 5CoxRuAl catalysts.

Acknowledgements

The authors would like to acknowledge the financial support of Korea Institute of Energy Technology Evaluation and Planning (KETEP) and GTL Technology Development Consortium (Korea National Oil Corp., Korea Gas Corp., Daelim Industrial Co., Ltd and Hyundai Engineering Co. Ltd) under "Energy Efficiency & Resources Programs" (Project No. 2006CCC11P011B) of the Ministry of Knowledge Economy, Republic of Korea.

References

[1] (a) J. Hong, P.A. Chernavskii, A.Y. Khodakov, W. Chu, Catal. Today 140 (2009) 135–141;
(b) G. Jacobs, A. Sarkar, Y. Ji, M. Luo, A. Dozier, B.H. Davis, Ind. Eng. Chem. Res. 47 (2008) 672–680;
(c) A.Y. Khodakov, W. Chu, P. Fongarland, Chem. Rev. 107 (2007) 1692–1744;
(d) W. Chu, L.N. Wang, P.A. Chernavskii, A. Khodakov, Angew. Chem. Int. Ed. 47 (2008) 5052–5055;
(e) J.-S. Girardon, E. Quinet, A. Griboval-Constant, P.A. Chernavskii, L. Gengembre, A.Y. Khodakov, J. Catal. 248 (2007) 143–157.
[2] P.J. van Berge, J. van de Loosdrechta, S. Barradas, A.M. van der Kraan, Catal. Today 58 (2000) 321–334.
[3] B. Jongsomjit, J. Panpranot, J.G. Goodwin Jr., J. Catal. 204 (2001) 98–109.
[4] B.A. Sexton, A.E. Hughes, T.W. Turneg, J. Catal. 97 (1986) 390–406.
[5] G. Jacobs, T.K. Das, Y. Zhang, J. Li, G. Racoillet, B.H. Davis, Appl. Catal. A 233 (2002) 263–281.
[6] E. Iglesia, Appl. Catal. A 161 (1997) 59–78.
[7] H. Xiong, Y. Zhang, K. Liew, J. Li, Fuel Process. Technol. 90 (2009) 237–246.
[8] Q. Cai, J. Li, Catal. Commun. 9 (2008) 2003–2006.
[9] Y.J. Lee, J.-Y. Park, K.W. Jun, J.W. Bae, P.S. Sai Prasad, Catal. Lett. 130 (2009) 198–203.
[10] S. Hammache, J.G. Goodwin Jr., R. Oukaci, Catal. Today 71 (2002) 361–367.
[11] A. Kogelbauer, J.G. Goodwin Jr., R. Oukaci, J. Catal 160 (1996) 125–133.
[12] S.H. Song, S.B. Lee, J.W. Bae, P.S. Sai Prasad, K.W. Jun, Catal. Commun. 9 (2008) 2282–2286.
[13] P. Li, J. Liu, N. Nag, P.A. Crozier, Appl. Catal. A 307 (2006) 212–221.
[14] G. Jacobs, P.M. Patterson, Y. Zhang, T. Das, J. Li, B.H. Davis, Appl. Catal. A 233 (2002) 215–226.
[15] A. Infantes-Molina, J. Merida-Robles, E. Rodriguez-Castellon, J.L.G. Fierro, A. Jimenez-Lopez, Appl. Catal. A 341 (2008) 35–42.
[16] S. Sun, K. Fujimoto, Y. Yoneyama, N. Tsubaki, Fuel 81 (2002) 1583–1591.
[17] J. Pampranot, J.G. Goodwin Jr., A. Sayari, Catal. Today 77 (2002) 269–284.
[18] L. Guczi, D. Bazin, I. Kovacs, L. Borko, Z. Schay, J. Lynch, P. Parent, C. Lafon, G. Stefler, Z. Koppany, I. Sajo, Top. Catal. 20 (2002) 129–139.
[19] G.L. Bezemer, J.H. Bitter, H.P.C.E. Kuipers, H. Oosterbeek, J.E. Holewijn, X. Xu, F. Kapteijn, A.J. van Dillen, K.P. de Jong, J. Am. Chem. Soc. 128 (2006) 3956–3964.
[20] J.W. Bae, I.G. Kim, J.S. Lee, K.H. Lee, E.J. Jang, Appl. Catal. A 240 (2003) 129–142.
[21] J. Zhang, J. Chen, J. Ren, Y. Sun, Appl. Catal. A 243 (2003) 121–133.
[22] E. Iglesia, S.C. Reyes, R.J. Madon, J. Catal. 129 (1991) 238–256.
[23] E. Iglesia, S.L. Soled, R.A. Fiato, G.H. Via, Stud. Surf. Sci. Catal. 81 (1994) 433–442.